The Journal of Geophysical Research: Atmospheres

Supporting Information for

Bulk Transfer Coefficients Estimated from Eddy-Covariance Measurements Over Lakes and Reservoirs

S. Guseva[1], F. Armani[2], A. R. Desai[3], N. L. Dias[4], T. Friborg[5], H. Iwata[6], J. Jansen[7,8], G. Lükő[9], I. Mammarella[10], I. Repina[11,12], A. Rutgersson[13], T. Sachs[14], K. Scholz[15], U. Spank[16], V. Stepanenko[12,17,18], P. Torma[9], T. Vesala[10,19], and A. Lorke[1]

[1] Institute for Environmental Sciences, University of Koblenz-Landau, Landau, Germany.
[2] Federal University of Paraná, Curitiba, PR, Brasil.
[3] Department of Atmospheric and Oceanic Sciences, University of Wisconsin-Madison, Madison, WI, USA.
[4] Department of Environmental Engineering, Federal University of Paraná, Curitiba, PR, Brasil.
[5] Department of Geosciences and Natural Resource Management, Oester Voldgade 10, 1350 Copenhagen K, Denmark.
[6] Department of Environmental Science, Faculty of Science, Shinshu University, Matsumoto, Japan.
[7] Department of Ecology and Genetics / Limnology, Uppsala University, Uppsala, Sweden.
[8] Département des Sciences Biologiques, Groupe de Recherche Interuniversitaire en Limnologie, Université du Québec à Montréal, Montréal, QC, Canada.
[9] Department of Hydraulic and Water Resources Engineering, Budapest University of Technology and Economics, Budapest, Hungary.
[10] Institute for Atmospheric and Earth System Research/Physics, Faculty of Science, University of Helsinki, Helsinki, Finland.
[11] A.M. Obukhov Institute of Atmospheric Physics, Moscow, Russia.
[12] Research Computing Center, Lomonosov Moscow State University, Moscow, Russia.
[13] Department of Earth Sciences, Uppsala University, Uppsala, Sweden.
[14] GFZ German Research Centre for Geosciences, Potsdam, Germany.
[15] Department of Ecology, University of Innsbruck, Innsbruck, Austria.
[16] Technische Universität Dresden, Faculty of Environmental Sciences, Institute of Hydrology and Meteorology, Chair of Meteorology, PF 1117, 01735 Tharandt, Germany.
[17] Faculty of Geography, Lomonosov Moscow State University, Moscow, Russia.
[18] Moscow Center of Fundamental and Applied Mathematics.
[19] Institute for Atmospheric and Earth System Research/Forest Sciences, Faculty of Agriculture and Forestry, University of Helsinki, Finland.
Corresponding author: Sofya Guseva (guseva@uni-landau.de)

Contents of this file

Text S1
Figures S1 to S11
Tables S1

Introduction

In the supporting information, we include text S1, table S1 and figures S1-S11 which are referred to Section 2.1 “Eddy-covariance measurements”, Section 2.2 “Data filtering” and Section 3 “Results”, respectively. Text S1 describes the effect of application different filters (Section 2.2) on the data. In particular, we selected two datasets from Lake Dagow and Lake Suwa which we consider representative for all other datasets. Moreover, in this text we explore different types of averaging over all datasets. Table S1 represents a short overview of the water bodies selected for the analysis and the data sources. Figures S1-S11 provide additional results related to the bulk transfer coefficients over lakes and reservoirs, known as drag coefficient (C_{DN}), Stanton number (C_{HN}) and Dalton number (C_{EN}). Figure S1 is a support for the fact that the drag coefficient at one individual bin (wind speed of 0.5 m s^{-1}) has a log-normal distribution. In addition, it shows that different kinds of averaging of the drag coefficient do not significantly affect the results. Figure S2 demonstrates the effect of the data filtering on the values of C_{DN} for one particular dataset (as an example, Lake Dagow, Germany). Figure S3 explores the effect of removing measurements that were potentially affected by floating vegetation in Lake Suwa (Japan). Figure S4a shows C_{DN} versus wind speed at 10 m height for all lakes and reservoirs. Lake Quinghai (China), Nam Theun 2 Reservoir (Laos) and Bol’shoi Vilyui Lake (Russia) were removed as they showed much larger or lower values in comparison to other water bodies of similar size. We did not find a reasonable explanation for that. In comparison with Figure 2a, Figure S4a shows less variability between the lakes. Figure S4b explores the difference between the Stanton numbers considering various types of water surface temperature: the skin temperature, the water temperature at some arbitrary depth or the mixture of both. Figure S5 provides all estimates of the transfer coefficients for the water bodies where obvious outliers are included. Figure S6 helps to understand the effect of the atmospheric stability on the transfer coefficients at wind speeds below 3 m s^{-1}. Figure S7 shows the fitting of the empirical function proposed for the measurements above the land for the Stanton and Dalton numbers. Figures S8, S10 demonstrate the relationship between the transfer coefficients and lake characteristics, including maximum fetch, maximum and mean water depth, and lake surface area. Figure S10 shows the dependence of the transfer coefficients on the measurement height. Figure S9 shows the results of a principal component analysis that was used to identify the possible relationship between C_{DN} and all predictors. Figure S11 provides evidence for the increase of the averaged wind speed with the increase of the lake surface area.

Text S1. Effect of data filtering and data averaging

Before analyzing the transfer coefficients for the combined datasets, we looked at data for each individual lake or reservoir. As a first step, we analyzed the dependence of the drag coefficient on U_{10}. It was apparent that the drag coefficients C_D (Eq. 2a) within individual wind speed intervals (0.5 m s^{-1} bin size) were nearly log-normally distributed. The Shapiro-Wilk test for logarithmically transformed data confirmed a normal distribution at a standard significance level of 0.05 for most of the bins (the example for one individual bin is shown for Lake Balaton, Hungary Figure S1a). The normalization of the drag coefficient to neutral atmospheric stability (C_{DN}) produced outliers (mainly for stable conditions), which affected the test results, but the distribution was still near log-normal. For our analysis, we consider bin-averaging of log-transformed data as an adequate measure to quantify the relation between the drag coefficient and wind speed. Some previous studies reported the median values of the drag coefficient (DeCosmo et al., 1996; Fairall et al., 2003), which are almost identical to the log-averaged values.

As there was no widely accepted way of presenting the transfer coefficients and their dependence on wind speed, we tested several statistical metrics. At first, we considered two types of representation of the transfer coefficients: the first way was to combine the data from all water bodies in each bin to estimate the mean value, logarithmic mean and median values. In the second approach, we calculated the same metrics but for already logarithmically bin averaged C_{DN} for each lake or reservoir. We did not consider arithmetic mean for the first method as the outliers strongly affected it. We found that the choice of other statistical metrics was not important due to the fact that, for example, the average percentage difference between the median of the first method (resulted in the lowest values of C_{DN}) and the standard mean of the second method (resulted in the highest values of C_{DN}) was around 20% (Figure S1b). We consider the second method and the logarithmic mean for further analysis as we observed near logarithmic distribution of the data in each bin.

To demonstrate the effect of data filtering (Section 2.2), we examined the longest dataset available to us, collected at the Lake Dagow site (Figure S2). The effects of applying the filters described below were nearly identical for any other dataset. Without any filtering, C_{DN} is characterized by large scatter, particularly, at low wind speeds (< 4 m s^{-1}) (Figure S2a). 3% of these data has been discarded after applying the quality check flags for unacceptable data. Removing wind directions (< 60°; > 90° and < 210; > 270°, see Table S1), considering the elongated shape of the lake, resulted in a slight decrease of the bin-averaged C_{DN}, except for the highest wind speed of 10 m s^{-1} (however, less data in bins were available there). A similar effect could be observed when the periods with ice cover were removed (Figure S2d). The bin-averaged C_{DN} appeared to be unaffected by removal of events with precipitation (Figure S2e). Removing data with $u_* < 0.05$ m s^{-1} resulted in increase of the bin-averaged C_{DN} at low wind speeds. In the case of Lake Dagow, C_{DN} for the first bin (U_{10} = 0-0.5 m s^{-1}) was a factor of 1.6 higher in comparison to C_{DN} without the u_* filter (Figure S2f). This selected threshold for the u_* filter is reported in literature, but is considered as arbitrary. Higher and lower values of this threshold result in higher and lower C_{DN} at low wind speeds. Following common practice, we applied the threshold of 0.05 m s^{-1} in the following analysis for all datasets. In general, the resulting filtered bin-averaged C_{DN} increased with decreasing wind speed at low wind speeds and remained at a relatively constant value of $3 \cdot 10^{-3}$ at wind speeds exceeding 3 m s^{-1} with a very slight increase at 9-10 m s^{-1}.

For their analysis, Andreas et al. (2005) and Li et al. (2016) removed the data with "unreasonable" values of the surface roughness length (e.g., $z_0 > 0.3$ m). We tested this criterion using our data (Figure S2g). While at high wind speeds (> 3 m s^{-1}) an increased surface roughness length could be attributed to the increasing height of the surface gravity waves, potential mechanism causing large roughness at low wind speed (e.g., z_0>1 m for Lake Dagow), remains unknown. Large values of z_0 has also been reported in Liu et al. (2020) for the measurements above land. Using this criterion to filter the data seemed to be inappropriate, as it mainly affected the drag coefficient at low wind speeds and simply cuts large values of C_{DN}. This filtering resulted in smaller bin-averaged C_{DN} at low wind speeds.

Filtering of the dataset from Lake Dagow resulted in a data reduction of approximately 73% (see details in the Table in the data repository 10.5281/zenodo.6597829 for other lakes or reservoirs). Lake Dagow is a relatively small lake (0.3 km^2) shielded with forest and may have larger scatter in the dependence of the drag coefficient on wind speed. However, we consider this example of filtering the data as representative for all other lakes and reservoirs under study as it contains most of applied filters and similar effects of filtering has been observed for other sites, as well as for C_{HN} and C_{EN}.

Removing the periods with floating vegetation on the water surface using the data from Lake Suwa did not significantly affect C_{DN} except at low wind speeds (< 2 m s^{-1}, Figure S3). Bin-averaged C_{DN} was slightly higher when applying this filter (the mean percentage difference was 16% for winds 0-2 m s^{-1}, Figure S3c).

Filtering of the datasets resulted in the total amount of filtered data ranging between 6.5 days (Lake Wohlen) and 5.3 years (Lake Taihu) with median value of 110 days for all datasets.

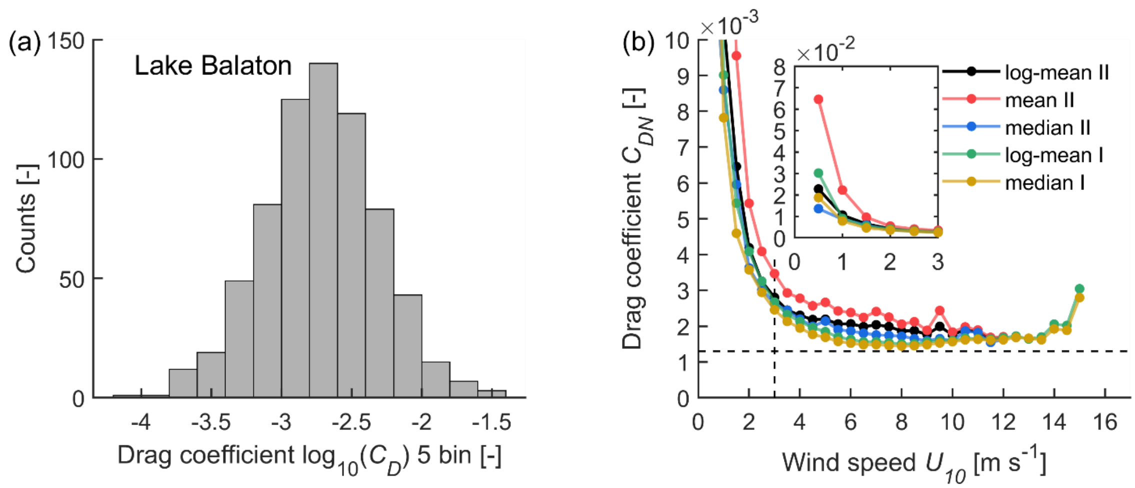

Figure S1. Histogram of log-transformed drag coefficients C_D (not accounting for atmospheric stability) for 5th bin corresponding to wind speed of 2.5 m s^{-1}. Data was collected at Lake Balaton site (Hungary, number of data points N = 694). A Shapiro-Wilk test of the log-transformed data confirmed a normal distribution at a standard significance level of 0.05. (b) Bin-averaged drag coefficients at neutral atmospheric stability (C_{DN}) estimated using the combined dataset as a function of U_{10}. Different colors refer to different averaging procedures: the first method (I) was to combine data from all water bodies in each bin of wind speeds and then estimate the logarithmic mean (black line with circles) and median (dark yellow line with circles) values (the arithmetic mean values without log-transformation are not shown because of their large scatter). For the second method (II), C_{DN} were logarithmically averaged for each lake before calculation of mean (red line and symbols), logarithmic mean (black), and median (blue) values.

The second method with logarithmic averaging was considered for further analysis. Small panel in (b) shows C_{DN} beyond the scale at low wind speeds.

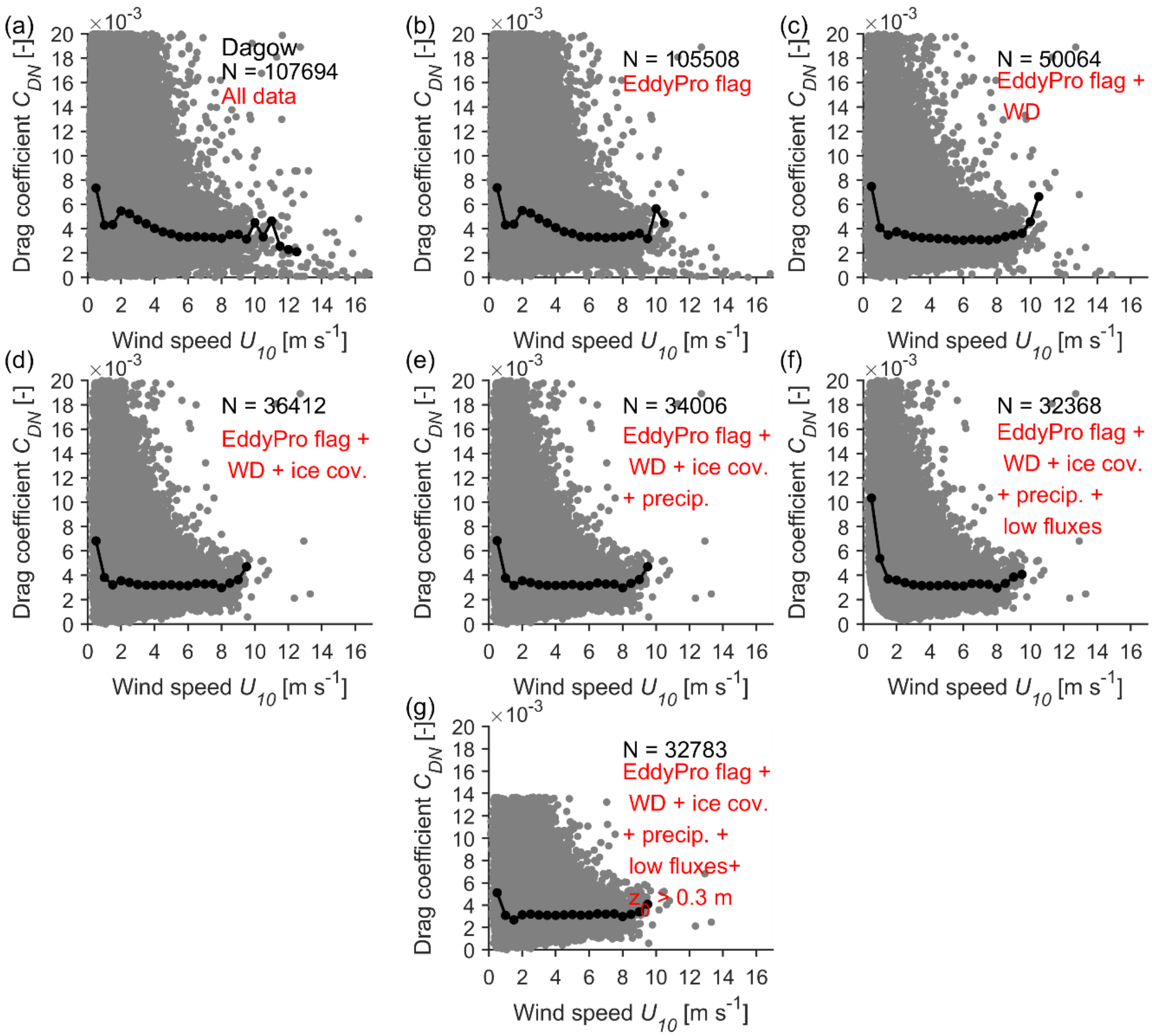

Figure S2. Effects of different steps of data filtering on estimated drag coefficients exemplified for the dataset from Lake Dagow (Germany). Neutral drag coefficients (C_{DN}) as a function of wind speed at 10 m height (U_{10}) are shown by grey dots that represent the estimates from individual 30 min flux measurements. The solid black line with circles shows logarithmic bin-averaged data in 0.5 m s^{-1} wind speed intervals. The number of data points (N) is indicated in the legend and a minimum of 10 data points was considered for bin-averaging. (a) No filtering was applied; (b) the data with quality flag equal to 2 indicating bad quality data (provided by EddyPro software, see details in Text S1) were removed; (c) wind directions (WD) were removed (60° < *WD* < 90°, 210° < *WD* < 270°), as the lake has an elongated shape, we considered the wind directions with the largest fetch; (d) the periods with ice cover were removed; (e) the periods with precipitation were removed; (f) low fluxes were removed ($u_* < 0.05$ m s^{-1}, $|H|, |E| < 10$ W m^{-2}); (g) removing the periods with surface roughness length $\mathbf{z_0 > 0.3}$ m.

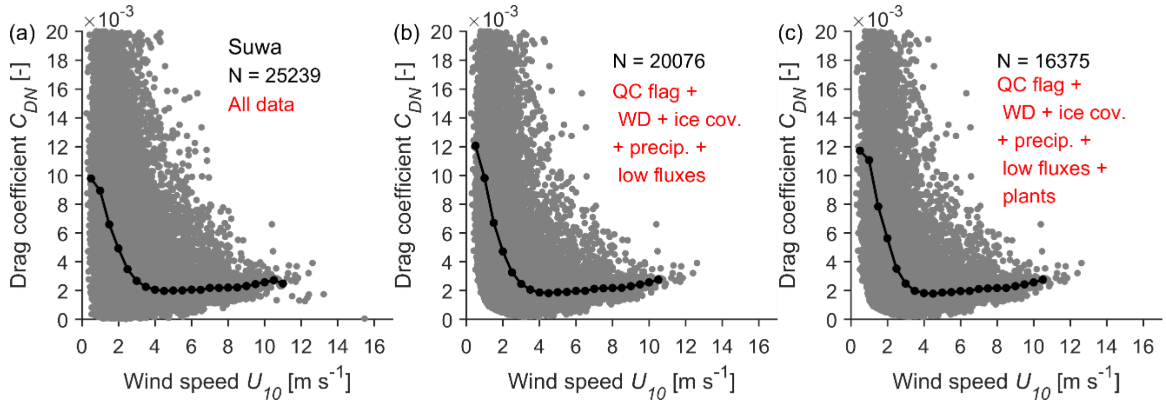

Figure S3. The effect of data filtering (similar to Figure S1): $\boldsymbol{C_{DN}}$ versus $\boldsymbol{U_{10}}$ for the dataset from Lake Suwa. (a) No filtering was applied; (b) all filters from Section 2.2 (except the periods with floating vegetation) were applied; (c) the periods with floating vegetation were removed (18.08.18-07.10.18; 15.05.19-09.09.19; 10.07.20-05.10.20).

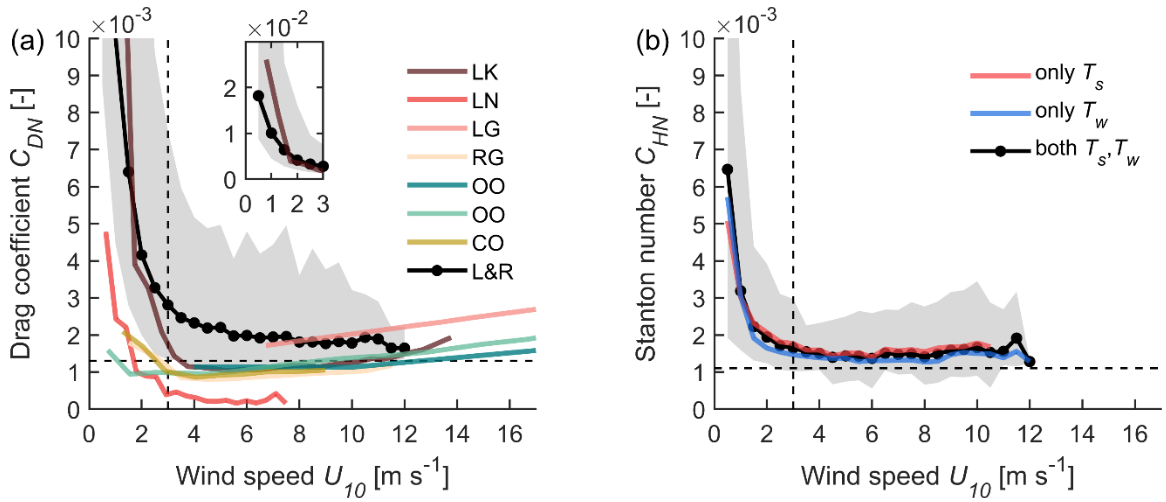

Figure S4. (a) $\boldsymbol{C_{DN}}$ versus $\boldsymbol{U_{10}}$. This panel is similar to Figure 2a except the fact that three additional lakes were excluded – Lake Quinghai (China), Nam Theun 2 Reservoir (Laos) and Bol'shoi Vilyui Lake (Russia). (b) Neutral Stanton number ($\boldsymbol{C_{HN}}$) versus $\boldsymbol{U_{10}}$. Three lines show bin averages of $\boldsymbol{C_{HN}}$ obtained using data with different measures of water temperature: skin temperature T_s (red line), bulk water temperature T_w (blue line) or both (black line with circles). Shaded grey area in both panels indicates data between the 5th and 95th percentiles.

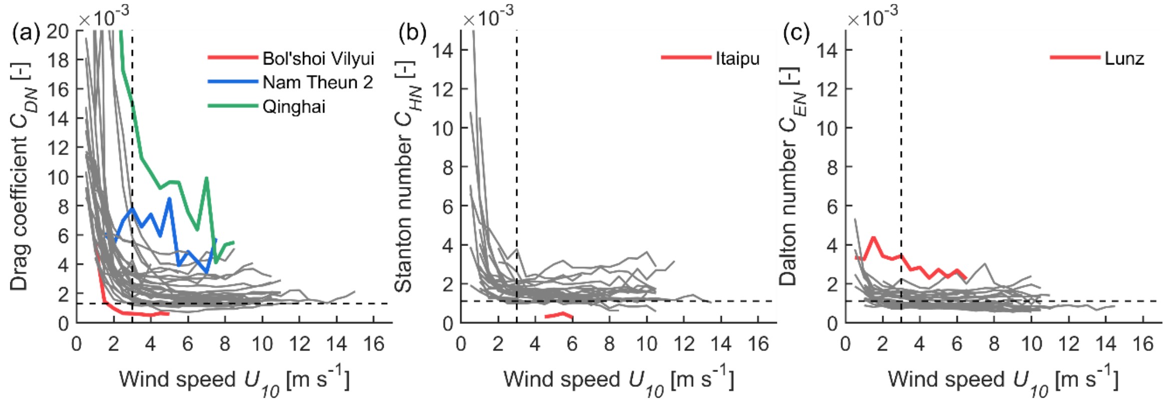

Figure S5. Neutral bin-averaged transfer coefficients (a) C_{DN}, (b) C_{HN}, (c) C_{EN} versus U_{10} are shown for all water bodies (grey lines). Thick colored lines (red, blue and green in (a) and red in (b) and (c)) show the water bodies which we marked as outliers, as their values were significantly larger or lower in comparison to other water bodies of similar size. Vertical and horizontal black dashed lines show a constant wind speed of 3 m s^{-1} and typical values of C_{DN}, C_{HN} = C_{EN} 1.3·10^{-3}, 1.1·10^{-3}, respectively. Note, the scale of Y-axis in (a) is different from (b) and (c) for better visibility.

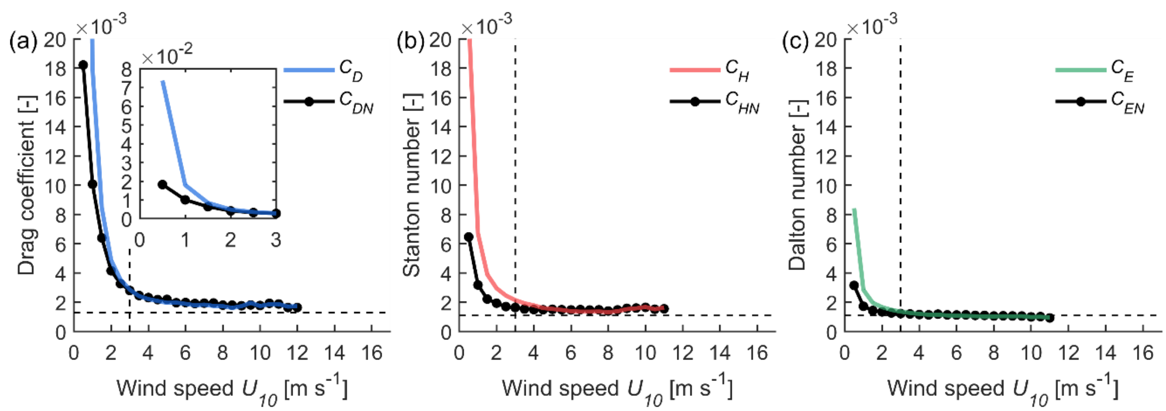

Figure S6. Comparison of the transfer coefficients (a) C_D, (b) C_H, (c) C_E (blue, red and green lines, respectively) with their counterparts adjusted for neutral atmospheric conditions C_{DN}, C_{HN}, C_{EN} (black line with circles) for bin-averaged values over all water bodies under study. Vertical and horizontal black dashed lines show a constant wind speed of 3 m s^{-1} and typical values of C_{DN}, C_{HN}= C_{EN} 1.3·10^{-3}, 1.1·10^{-3}, respectively. The smaller panel in (a) shows the drag coefficient for wind speeds less than 3 m s^{-1} at enlarged scale. It is apparent that atmospheric stability affected the transfer coefficients at low wind speeds only.

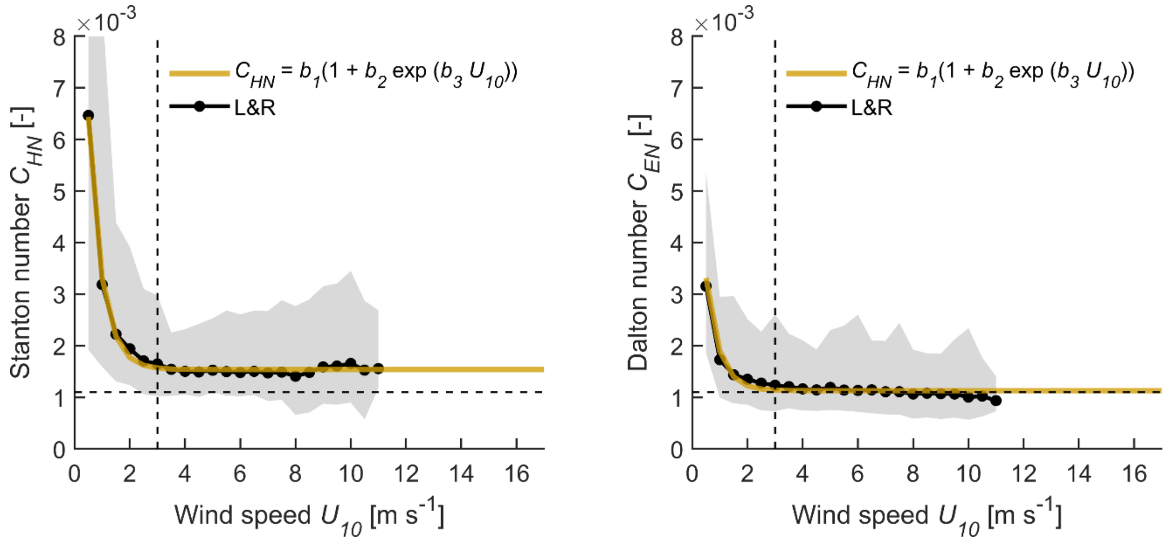

Figure S7. Neutral (a) Stanton number, (b) Dalton number marked by black line with symbols (similar to Figure 4a in the manuscript). The dark yellow line shows the function $C = b_1[1 + b_2\exp(b_3U_{10})]$ proposed by Liu et al., (2020) with the fitted coefficients b_1 = 1.5·10^{-3}; b_2 = 8.8; b_3 = -2 for Stanton number and b_1 = 1.1·10^{-3}; b_2 = 5.5; b_3 = -2.1 for Dalton number (see details in Section 3.2). Vertical and horizontal black dashed lines show a constant wind speed of 3 m s^{-1} and typical value of $C_{HN} = C_{EN}$ being equal to 1.1·10^{-3}.

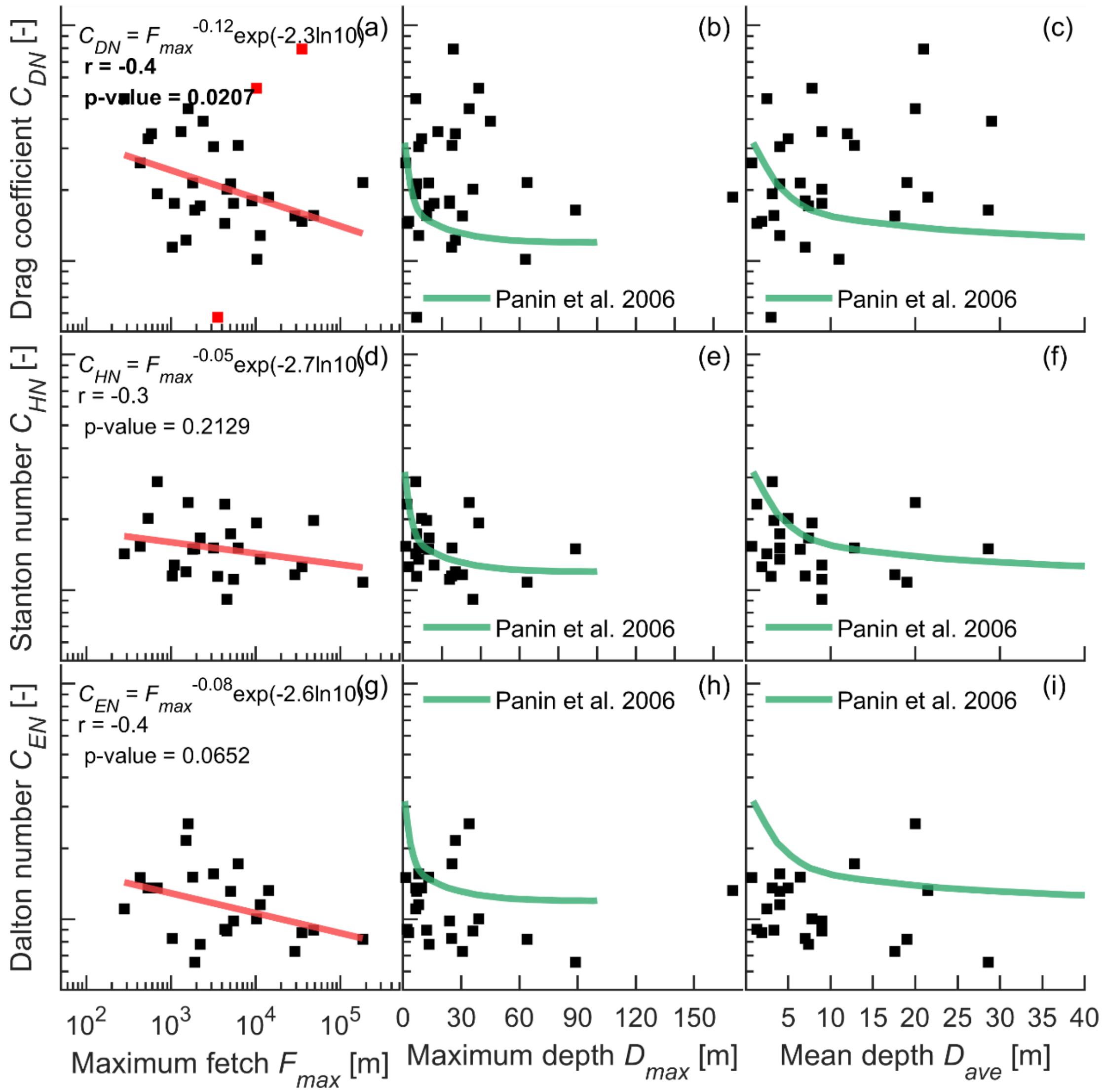

Figure S8. Mean neutral transfer coefficients (a, b, c) C_{DN}; (d, e, f) C_{HN}; (g, h, i) C_{EN} versus maximum fetch, maximum and average water depth of the water body. All plots show the exchange coefficients averaged for wind speeds exceeding 3 m s^{-1}. Each black square on the panels is the value of the transfer coefficient for one lake or reservoir. Red line in all plots shows linear regression in logarithmic domain ($\log_{10}y = A\log_{10}x + B$). The relationship between the transfer coefficients and selected lake characteristics is expressed as a power dependence $y = x^A\exp(B\ln10)$, where A and B are the slope and intercept of the linear regression. Corresponding slope and intercept as well as the Pearson correlation coefficient and p-value are written at left upper corner of the plot. Three red squares in (a), (b) correspond to Lake Quinghai, Nam Theun 2 Reservoir and and Bol'shoi Vilyui Lake were not considered for linear regression analysis of the drag coefficient and the Pearson correlation for the drag coefficient. Green line illustrates the result from (Panin et al., 2006). There is a weak negative correlation between the Stanton and Dalton numbers and maximum fetch as well as a significant negative correlation between the drag coefficient and maximum fetch. No evidence for any kind of relationship between all transfer coefficients and maximum or average water depth was found.

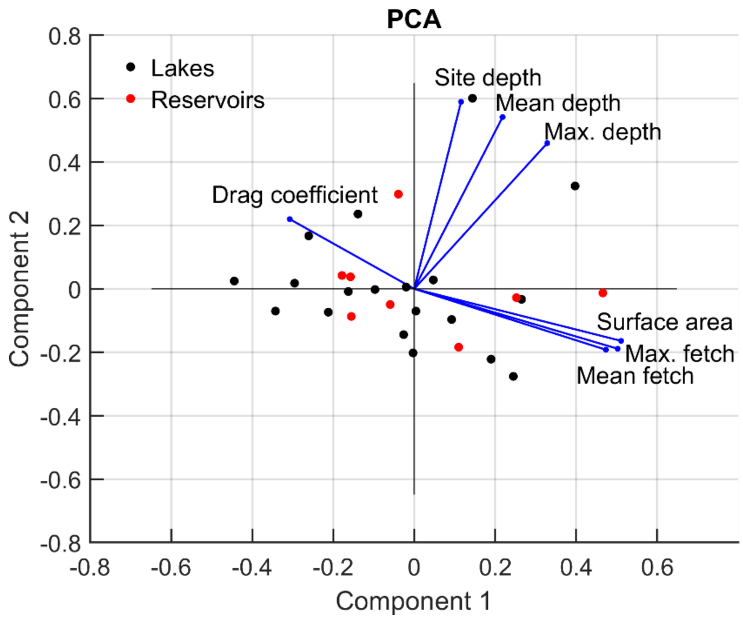

Figure S9. Principal component analysis for the data shown by black and red dots corresponding to the lakes and reservoirs, respectively. Representations of the original predictors in the first two principal component basis are presented with blue lines with dots. The fact that the drag coefficient and different types of the depths are nearly orthogonal to each other indicates that there is no correlation between them.

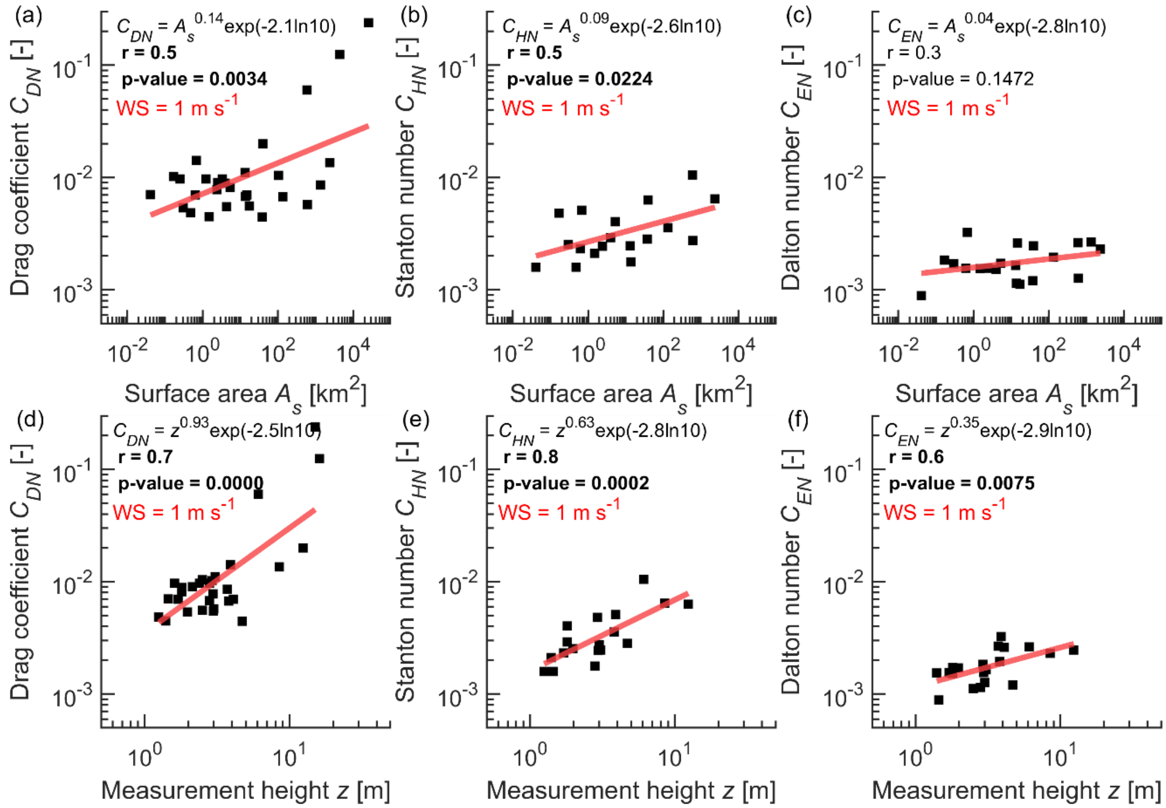

Figure S10. Mean neutral drag coefficient as a function of (a), (b), (c) lake surface area; (d), (e), (f) measurement height (if it changed – the average height for the measurement period was taken) at a fixed wind speed of 1 m s^{-1} (shown as "WS = 1 m s^{-1}"). Each black square on the panels represents the mean value of the drag coefficient for one lake or reservoir. Red line in all plots shows linear regression in logarithmic domain $\log_{10}y = A\log_{10}x + B$. The relationship between the transfer coefficients and selected lake characteristics is expressed as a power dependence $y = x^A \exp(B\ln 10)$, where A and B are the slope and intercept of the linear regression (shown in the upper left corner). Corresponding Pearson correlation coefficient and p-value are written at left upper corner of the plot. A significant positive correlation (marked by bold font) was found between C_{DN} , C_{HN} and surface area as well as measurement height (also C_{EN}).

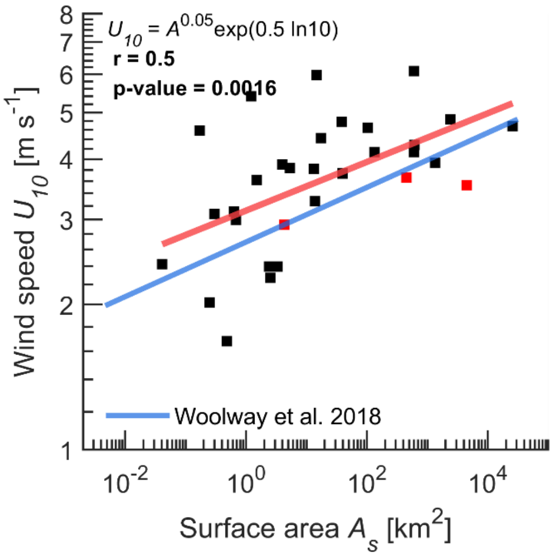

Figure S11. Relationship between the averaged wind speed estimated for all water bodies and the surface area. Red line in all plots shows linear regression in logarithmic domain. The blue line represents the results reported in (Woolway et al., 2018). The relationship between the wind speed and lake surface area is expressed as a power dependence written at left upper corner of the panel. The Pearson correlation coefficient and p-value are written at left upper corner of the panel. Three red squares correspond to Lake Quinghai, Nam Theun 2 Reservoir and and Bol'shoi Vilyui Lake but they were not excluded for this regression analysis.

Table S1. Lake and reservoirs under study and their characteristics. Corresponding datasets and information about their processing.

	Lake/Reservoir	Area A_s [km^2]	Mean/Max depth	Country	Filters	Accepted wind directions [°]	Publication	Data repository
1	Acton Lake (Reservoir)	0.12	- / 9.3	USA	QCF(2); WD; IC; LF	until 04.05.18: < 170; after: < 15 and > 300; > 130 and < 205	(Waldo et al., 2021)	(Waldo et al., 2021)
2	Lake Balaton	596	3.3 / 12.2	Hungary	QCF(≥ 6); LF	All	(Lükő et al., 2020, 2022)	https://zenodo.org/record/5597141#.YbIcK71_pPY
3	Bautzen Reservoir	5.3	7.4 / 13.5	Germany	WD; LF	> 195 and < 355	(Guseva et al., 2021)	***Data available from Uwe Spank
4	Bol'shoi Vilyui Lake	4.3	3 / 7	Russia	LF	All	(Stepanenko et al., 2018)	***Data available from Irina Repina
5	Lake Dagow	0.3	5 / 9.5	Germany	QCF(2); WD; IC; P; LF	> 60 and < 90; < 270 and > 210	(Guseva et al., 2021)	https://doi.org/10.18140/FLX/1669633
6	Daring Lake	14.8	- / 27	Canada	P; LF	* < 10 and > 270	(Golub et al., 2021)	(Golub et al., 2022)
7	Douglas Lake	13.7	9 / 24	USA	LF	* < 180 and > 270	(Morin et al., 2018; Golub et al., 2021)	
8	Eastmain Reservoir	602	11 / 63	Canada	WD; IC; P; LF	> 180 and < 330	(Demarty et al., 2011; Golub et al., 2021)	
9	Lake Erie	$2.6 \cdot 10^4$	19 / 64	USA	IC; P; LF	All	(Shao et al., 2015; Golub et al., 2021b)	
10	Itaipu Reservoir	$1.4 \cdot 10^3$	21.5 / 170	Brazil	WD; LF	< 30 and > 140	(Armani et al., 2020)	***Data available from Fernando Armani
11	Lake Klöntal	3.3	29 / 45	Switzerland	WD; LF	> 75 and < 243	(Sollberger et al., 2017)	***Data available from Werner Eugster
12	Lake Kuivajärvi	0.63	6.4 / 13.2	Finland	WD; P; LF	> 135 and < 185; > 315	(Heiskanen et al., 2015; Mammarella et al., 2015; Golub et al., 2021)	(Golub et al., 2022)
13	Lake Lunz	0.68	20 / 34	Austria	QCF(2); WD; IC; P; LF	> 195 and < 355	(Scholz et al., 2021)	https://doi.org/10.5281/zenodo.4519167
14	Lake Mendota	39.4	12.8/25.3	USA	WD; IC; P; LF	< 30; > 285		(Desai, 2018)
15	Nam Theun 2 Reservoir	450	7.8/39	Laos	P; LF; T	All	(Deshmukh et al., 2014)	(Golub et al., 2022)

16	Lake Ngoring	610.7	17.6/30.7	China	WD; LF	> 53 and < 175	(Han, 2020; Han et al., 2020)	https://dataverse.harvard.edu/dataset.xhtml?persistentId=doi:10.7910/DVN/SRIAYJ;
17	Lake Pallasjärvi	17.2	9/36	Finland	P; LF	* < 60 and > 180	(Lohila et al., 2015; Golub et al., 2021)	(Golub et al., 2022)
18	Lake Qinghai	$4.4\cdot10^{3}$	21/26	China	WD; LF	< 110 and > 325	(Li et al., 2016; Li et al., 2018)	https://data.tpdc.ac.cn/en/data/1df8f705-8a98-4ede-8de7-d065f7f674bd/
19	Rappbode Reservoir	4	28.6/89	Germany	WD; LF	> 180 and < 240	(Spank et al., 2020)	***Data available from Uwe Spank
20	Ross Barnett Reservoir	134	4/8	USA	P; LF	All	(Liu et al., 2009)	(Golub et al., 2022)
21	Lake Rotsee	0.48	9/16	Switzerland	WD; LF	> 7 and < 65; > 235 and < 262	(Schubert et al., 2012)	***Data available from Werner Eugster
22	Siberian Lake	1.21	3.1/6.5	Russia	QCF(2); IC; LF; T	All	(Franz et al., 2018)	***Data available from Torsten Sachs
23	Lake Soppensee	0.25	12/27	Switzerland	LF	All	(Eugster, 2003)	***Data available from Werner Eugster
24	Lake Suwa	13.3	4/6.9	Japan	QCF(≥ 6); WD; IC; LC; P; LF	< 5 and > 240	(Iwata et al., 2018, 2020)	http://asiaflux.net/index.php?page_id=1355
25	Lake Taihu	$2.4\cdot10^{3}$	1.9/3	China	QCF(2); LF	All *Data from PTS point only	(Zhang et al., 2020)	https://dataverse.harvard.edu/dataset.xhtml?persistentId=doi:10.7910/DVN/HEWCWM
26	Lake Tämnaren	38	1.3/2	Sweden	WD; IC; LF	> 120 and < 333	(Podgrajsek et al., 2014; Sahlée et al., 2014)	(Golub et al., 2022)
27	Lake Toolik	1.5	7/25	USA	P; LF	All	(Eugster et al., 2020; Golub et al., 2021)	
28	Lake Valkea Kotinen	$4.1\cdot10^{-2}$	2.5/-	Finland	WD; P; LF	> 134 and < 180; > 300 and < 350	(Nordbo et al., 2011; Golub et al., 2021)	
29	Lake Vanajavesi	103	7/24	Finland	IC; LF	All	(Salgado et al., 2016; Golub et al., 2021)	

30	Lake Villasjön	0.17	0.7/1.3	Sweden	WD; IC; LF	> 10 and < 75; > 114 and < 140	(Jammet et al., 2017; Jansen et al., 2019)	http://www.europe-fluxdata.eu/page21/site-details?id=SE-St1
31	Lake Wohlen (Reservoir)	2.5	9/18	Switzerland	WD;LF	> 245	(Eugster et al., 2011)	***Data available from Werner Eugster

*QCF(2 or ≥ 6): removing unacceptable data with quality check flags equal to 2 (EddyPro software,(LI-COR, Inc, 2021)) and ≥ 6 (Eddy-covariance software TK3,(Mauder & Foken, 2015)) (Foken et al., 2012); WD: limitation of the wind directions (site-specific); IC: removing periods with ice cover; P: removing periods with precipitation; LF: removing low fluxes ($\boldsymbol{u}_*$<0.05 m s^{-1}, $|\boldsymbol{H}|$, $|\boldsymbol{E}|$<10 W m^{-2}); L: removing periods with floating vegetation on the water surface (18.08.18-07.10.18; 15.05. 2019-09.09.2019; 10.07.20-05.10.20, Lake Suwa, Japan); T: removing periods with low water level (appearance of many small islands around the measurement location in Nam Theun 2 Reservoir) or removing periods when footprint was on the shore (Siberian Lake)

* Wind directions were removed by the owners of the dataset.

References

Armani, F. A. S., Dias, N. L., & Damázio, J. M. (2020). Eddy-covariance CO2 fluxes over Itaipu lake, southern Brazil. *RBRH*, *25*, e43. https://doi.org/10.1590/2318-0331.252020200060

Demarty, M., Bastien, J., & Tremblay, A. (2011). Annual follow-up of gross diffusive carbon dioxide and methane emissions from a boreal reservoir and two nearby lakes in Québec, Canada. *Biogeosciences*, *8*(1), 41–53. https://doi.org/10.5194/bg-8-41-2011

Desai, A. (2018). *AmeriFlux AmeriFlux US-Pnp Lake Mendota, Picnic Point Site* [Data set]. AmeriFlux; University of Wisconsin Madison. https://doi.org/10.17190/AMF/1433376

Deshmukh, C., Serça, D., Delon, C., Tardif, R., Demarty, M., Jarnot, C., Meyerfeld, Y., Chanudet, V., Guédant, P., Rode, W., Descloux, S., & Guérin, F. (2014). Physical controls on CH₄ emissions from a newly flooded subtropical freshwater hydroelectric reservoir: Nam Theun 2. *Biogeosciences*, *11*(15), 4251–4269. https://doi.org/10.5194/bg-11-4251-2014

Eugster, W. (2003). CO_2 exchange between air and water in an Arctic Alaskan and midlatitude Swiss lake: Importance of convective mixing. *Journal of Geophysical Research*, *108*(D12), 4362. https://doi.org/10.1029/2002JD002653

Eugster, W., DelSontro, T., Shaver, G. R., & Kling, G. W. (2020). Interannual, summer, and diel variability of CH_4 and CO_2 effluxes from Toolik Lake, Alaska, during the ice-free periods 2010–2015. *Environmental Science: Processes & Impacts*, 10.1039.D0EM00125B. https://doi.org/10.1039/D0EM00125B

Eugster, W., DelSontro, T., & Sobek, S. (2011). *Eddy covariance flux measurements confirm extreme CH₄ emissions from a Swiss hydropower reservoir and resolve their short-term variability* [Preprint]. Biogeochemistry: Greenhouse Gases. https://doi.org/10.5194/bgd-8-5019-2011

Foken, T., Leuning, R., Oncley, S. R., Mauder, M., & Aubinet, M. (2012). Corrections and Data Quality Control. In M. Aubinet, T. Vesala, & D. Papale (Eds.), *Eddy Covariance* (pp. 85–131). Springer Netherlands. https://doi.org/10.1007/978-94-007-2351-1_4

Franz, D., Mammarella, I., Boike, J., Kirillin, G., Vesala, T., Bornemann, N., Larmanou, E., Langer, M., & Sachs, T. (2018). Lake-Atmosphere Heat Flux Dynamics of a Thermokarst Lake in Arctic Siberia. *Journal of Geophysical Research: Atmospheres*, *123*(10), 5222–5239. https://doi.org/10.1029/2017JD027751

Golub, M., Desai, A. R., Vesala, T., Mammarella, I., Ojala, A., Bohrer, G., Weyhenmeyer, G. A., Blanken, P. D., Eugster, W., Koebsch, F., Chen, J., Czajkowski, K. P., Deshmukh, C., Guérin, F., Heiskanen, J. J., Humphreys, E. R., Jonsson, A., Karlsson, J., Kling, G. W., … Xiao, W. (2021a). *New insights into diel to interannual variation in carbon dioxide emissions from lakes and reservoirs* [Preprint]. Environmental Sciences. https://doi.org/10.1002/essoar.10507313.1

Golub, M., Desai, A. R., Vesala, T., Mammarella, I., Ojala, A., Bohrer, G., Weyhenmeyer, G. A., Blanken, P. D., Eugster, W., Koebsch, F., Chen, J., Czajkowski, K. P., Deshmukh, C., Guérin, F., Heiskanen, J. J., Humphreys, E. R., Jonsson, A., Karlsson, J., Kling, G. W., … Xiao, W. (2021b). *New insights into diel to interannual variation in carbon dioxide emissions from lakes and reservoirs* [Preprint]. Environmental Sciences. https://doi.org/10.1002/essoar.10507313.1

Golub, M., Desai, A. R., Vesala, T., Mammarella, I., Ojala, A., Bohrer, G., Weyhenmeyer, G., Blanken, P., Eugster, W., Franz, D., Koebsch, F., Chen, J., Czajkowski, K., Deshmukh, C. S., Elbers, J., Friborg, T., Glatzel, S., Guerin, F., Heiskanen, J., … Xiao, W. (2022). *Half-hourly gap-filled Northern Hemisphere lake and reservoir carbon flux and micrometeorology, 2006—2015* [Data set]. Environmental Data Initiative. https://doi.org/10.6073/PASTA/87A35CA843D8739D75882520C724E99E

Guseva, S., Casper, P., Sachs, T., Spank, U., & Lorke, A. (2021). Energy Flux Paths in Lakes and Reservoirs. *Water*, *13*(22), 3270. https://doi.org/10.3390/w13223270

Han, B. (2020). *Eddy covariance data in Ngoring Lake in Tibet from 2011 to 2013* [Data set]. Harvard Dataverse. https://doi.org/10.7910/DVN/SRIAYJ

Han, B., Meng, X., Yang, Q., Wu, R., Lv, S., Li, Z., Wang, X., Li, Y., & Yu, L. (2020). Connections Between Daily Surface Temperature Contrast and CO_2 Flux Over a Tibetan Lake: A Case Study of Ngoring Lake. *Journal of Geophysical Research: Atmospheres*, *125*(6). https://doi.org/10.1029/2019JD032277

Heiskanen, J. J., Mammarella, I., Ojala, A., Stepanenko, V., Erkkilä, K., Miettinen, H., Sandström, H., Eugster, W., Leppäranta, M., Järvinen, H., Vesala, T., & Nordbo, A. (2015). Effects of water clarity on lake stratification and lake-atmosphere heat exchange. *Journal of Geophysical Research: Atmospheres*, *120*(15), 7412–7428. https://doi.org/10.1002/2014JD022938

Iwata, H., Hirata, R., Takahashi, Y., Miyabara, Y., Itoh, M., & Iizuka, K. (2018). Partitioning Eddy-Covariance Methane Fluxes from a Shallow Lake into Diffusive and Ebullitive Fluxes. *Boundary-Layer Meteorology*, *169*(3), 413–428. https://doi.org/10.1007/s10546-018-0383-1

Iwata, H., Nakazawa, K., Sato, H., Itoh, M., Miyabara, Y., Hirata, R., Takahashi, Y., Tokida, T., & Endo, R. (2020). Temporal and spatial variations in methane emissions from the littoral zone of a shallow mid-latitude lake with steady methane bubble emission areas. *Agricultural and Forest Meteorology*, *295*, 108184. https://doi.org/10.1016/j.agrformet.2020.108184

Jammet, M., Dengel, S., Kettner, E., Parmentier, F.-J. W., Wik, M., Crill, P., & Friborg, T. (2017). Year-round CH₄ and CO₂ flux dynamics in two contrasting freshwater ecosystems of the subarctic. *Biogeosciences*, *14*(22), 5189–5216. https://doi.org/10.5194/bg-14-5189-2017

Jansen, J., Thornton, B. F., Jammet, M. M., Wik, M., Cortés, A., Friborg, T., MacIntyre, S., & Crill, P. M. (2019). Climate-Sensitive Controls on Large Spring Emissions of CH_4 and CO_2 From Northern Lakes. *Journal of Geophysical Research: Biogeosciences*, *124*(7), 2379–2399. https://doi.org/10.1029/2019JG005094

Li, X., Yang, X., Ma, Y., Hu, G., Hu, X., Wu, X., Wang, P., Huang, Y., Cui, B., & Wei, J. (2018). Qinghai Lake Basin Critical Zone Observatory on the Qinghai-Tibet Plateau. *Vadose Zone Journal*, *17*(1), 180069. https://doi.org/10.2136/vzj2018.04.0069

Li, X.-Y., Ma, Y.-J., Huang, Y.-M., Hu, X., Wu, X.-C., Wang, P., Li, G.-Y., Zhang, S.-Y., Wu, H.-W., Jiang, Z.-Y., Cui, B.-L., & Liu, L. (2016). Evaporation and surface energy budget over the largest high-altitude saline lake on the Qinghai-Tibet Plateau: WATER AND ENERGY FLUX OVER QINGHAI LAKE. *Journal of Geophysical Research: Atmospheres*, *121*(18), 10,470-10,485. https://doi.org/10.1002/2016JD025027

LI-COR, Inc. (2021). *EddyPro® Software (Version 7.0)*. LI-COR. https://www.licor.com/env/support/EddyPro/home.html

Liu, C., Li, Y., Gao, Z., Zhang, H., Wu, T., Lu, Y., & Zhang, X. (2020). Improvement of Drag Coefficient Calculation Under Near-Neutral Conditions in Light Winds Over land. *Journal of Geophysical Research: Atmospheres*, *125*(24). https://doi.org/10.1029/2020JD033472

Liu, H., Zhang, Y., Liu, S., Jiang, H., Sheng, L., & Williams, Q. L. (2009). Eddy covariance measurements of surface energy budget and evaporation in a cool season over southern open water in Mississippi. *Journal of Geophysical Research*, *114*(D4), D04110. https://doi.org/10.1029/2008JD010891

Lohila, A., Tuovinen, J. P., Hatakka, J., Aurela, M., Vuorenmaa, J., Haakana, M., & Laurila, T. (2015). *Carbon dioxide and energy fluxes over a northern boreal lake*. *20*(4), 474–488.

Lükő, G., Torma, P., Krámer, T., Weidinger, T., Vecenaj, Z., & Grisogono, B. (2020). Observation of wave-driven air–water turbulent momentum exchange in a large but fetch-limited shallow lake. *Advances in Science and Research*, *17*, 175–182. https://doi.org/10.5194/asr-17-175-2020

Lükő, G., Torma, P., & Weidinger, T. (2022). Intra-Seasonal and Intra-Annual Variation of the Latent Heat Flux Transfer Coefficient for a Freshwater Lake. *Atmosphere*, *13*(2), 352. https://doi.org/10.3390/atmos13020352

Mammarella, I., Nordbo, A., Rannik, Ü., Haapanala, S., Levula, J., Laakso, H., Ojala, A., Peltola, O., Heiskanen, J., Pumpanen, J., & Vesala, T. (2015). Carbon dioxide and energy fluxes over a small boreal lake in Southern Finland: CO_2 and Energy Fluxes Over Lake. *Journal of Geophysical Research: Biogeosciences*, *120*(7), 1296–1314. https://doi.org/10.1002/2014JG002873

Mauder, M., & Foken, T. (2015). *Eddy-Covariance Software TK3*. Zenodo. https://doi.org/10.5281/ZENODO.20349

Morin, T. H., Rey-Sánchez, A. C., Vogel, C. S., Matheny, A. M., Kenny, W. T., & Bohrer, G. (2018). Carbon dioxide emissions from an oligotrophic temperate lake: An eddy covariance approach. *Ecological Engineering*, *114*, 25–33. https://doi.org/10.1016/j.ecoleng.2017.05.005

Nordbo, A., Launiainen, S., Mammarella, I., Leppäranta, M., Huotari, J., Ojala, A., & Vesala, T. (2011). Long-term energy flux measurements and energy balance over a small boreal lake using eddy covariance technique. *Journal of Geophysical Research*, *116*(D2), D02119. https://doi.org/10.1029/2010JD014542

Panin, G. N., Nasonov, A. E., & Foken, T. (2006). Evaporation and heat exchange of a body of water with the atmosphere in a shallow zone. *Izvestiya, Atmospheric and Oceanic Physics*, *42*(3), 337–352. https://doi.org/10.1134/S0001433806030078

Podgrajsek, E., Sahlée, E., Bastviken, D., Holst, J., Lindroth, A., Tranvik, L., & Rutgersson, A. (2014). Comparison of floating chamber and eddy covariance measurements of lake greenhouse gas fluxes. *Biogeosciences*, *11*(15), 4225–4233. https://doi.org/10.5194/bg-11-4225-2014

Sahlée, E., Rutgersson, A., Podgrajsek, E., & Bergström, H. (2014). Influence from Surrounding Land on the Turbulence Measurements Above a Lake. *Boundary-Layer Meteorology*, *150*(2), 235–258. https://doi.org/10.1007/s10546-013-9868-0

Salgado, R., Potes, M., Mammarella, I., & Provenzale, M. (2016). *Measurements of Mass, Momentum and Energy fluxes over an ice/snow covered lake*. EGU.

Scholz, K., Ejarque, E., Hammerle, A., Kainz, M., Schelker, J., & Wohlfahrt, G. (2021). Atmospheric CO_2 Exchange of a Small Mountain Lake: Limitations of Eddy Covariance and Boundary Layer Modeling Methods in Complex Terrain. *Journal of Geophysical Research: Biogeosciences*, *126*(7). https://doi.org/10.1029/2021JG006286

Schubert, C. J., Diem, T., & Eugster, W. (2012). Methane Emissions from a Small Wind Shielded Lake Determined by Eddy Covariance, Flux Chambers, Anchored Funnels, and Boundary Model Calculations: A Comparison. *Environmental Science & Technology*, *46*(8), 4515–4522. https://doi.org/10.1021/es203465x

Shao, C., Chen, J., Stepien, C. A., Chu, H., Ouyang, Z., Bridgeman, T. B., Czajkowski, K. P., Becker, R. H., & John, R. (2015). Diurnal to annual changes in latent, sensible heat, and CO_2 fluxes over a Laurentian Great Lake: A case study in Western Lake Erie. *Journal of Geophysical Research: Biogeosciences*, *120*(8), 1587–1604. https://doi.org/10.1002/2015JG003025

Sollberger, S., Wehrli, B., Schubert, C. J., DelSontro, T., & Eugster, W. (2017). Minor methane emissions from an Alpine hydropower reservoir based on monitoring of diel and seasonal variability. *Environmental Science: Processes & Impacts*, *19*(10), 1278–1291. https://doi.org/10.1039/C7EM00232G

Spank, U., Hehn, M., Keller, P., Koschorreck, M., & Bernhofer, C. (2020). A Season of Eddy-Covariance Fluxes Above an Extensive Water Body Based on Observations from a Floating Platform. *Boundary-Layer Meteorology*, *174*(3), 433–464. https://doi.org/10.1007/s10546-019-00490-z

Stepanenko, V. M., Repina, I. A., Artamonov, A. Y., Gorin, S. L., Lykossov, V. N., & Kulyamin, D. V. (2018). Mid-depth temperature maximum in an estuarine lake. *Environmental Research Letters*, *13*(3), 035006. https://doi.org/10.1088/1748-9326/aaad75

Waldo, S., Beaulieu, J. J., Barnett, W., Balz, D. A., Vanni, M. J., Williamson, T., & Walker, J. T. (2021). Temporal trends in methane emissions from a small eutrophic reservoir: The key role of a spring burst. *Biogeosciences*, *18*(19), 5291–5311. https://doi.org/10.5194/bg-18-5291-2021

Woolway, R. I., Verburg, P., Lenters, J. D., Merchant, C. J., Hamilton, D. P., Brookes, J., Eyto, E., Kelly, S., Healey, N. C., Hook, S., Laas, A., Pierson, D., Rusak, J. A., Kuha, J., Karjalainen, J., Kallio, K., Lepistö, A., & Jones, I. D. (2018). Geographic and temporal variations in turbulent heat loss from lakes: A global analysis across 45 lakes. *Limnology and Oceanography*, *63*(6), 2436–2449. https://doi.org/10.1002/lno.10950

Zhang, Z., Zhang, M., Cao, C., Wang, W., Xiao, W., Xie, C., Chu, H., Wang, J., Zhao, J., Jia, L., Liu, Q., Huang, W., Zhang, W., Lu, Y., Xie, Y., Wang, Y., Pu, Y., Hu, Y., Chen, Z., … Lee, X. (2020). *A dataset of microclimate and radiation and energy fluxes from the Lake Taihu Eddy Flux Network* [Data set]. Harvard Dataverse. https://doi.org/10.7910/DVN/HEWCWM